Reliability Engineering and System Safety 250 (2024) 110304

Contents lists available at ScienceDirect

Reliability Engineering and System Safety

journal homepage: www.elsevier.com/locate/ress

Cascading structural failures of towers in an electric power transmission line due to straight line winds

Saransh Dikshit, Ian Dobson, Alice Alipour *

Iowa State University, Ames IA, United States

ARTICLE INFO

Keywords:
Cascading failure risk
Probability
Transmission tower
Structural failure
Wind
Resilience engineering

ABSTRACT

The bulk electricity that powers our society flows along high voltage transmission lines that are conducting cables hung with insulators from a series of transmission towers. High winds can damage these structures and the loss of the transmission line sometimes causes a blackout. When a tower structurally fails, the adjacent towers have unbalanced load, and are more likely to fail, so there is a cascading effect by which tower failures can lead to further tower failures.

This paper analyzes the cascading failures of towers due to extreme straight line winds. A dynamic analysis of the transmission tower–insulator–conductor system under wind loads yields fragility curves that describe the probability of structural failure for both intact and failed adjacent towers. The paper then derives novel mathematical formulas for the probabilities of the number of towers that fail. The new formulas apply generally to cascading failure along a line of general components. The calculations use generating functions and computer algebra, and account for the interspersed anchor towers that are strongly built to withstand high winds. The effect of cascading on the number of towers failed and the life cycle cost is quantified in a case study of a transmission line with twenty-five towers.

1. Introduction

High voltage transmission lines are part of the vital electrical infrastructure conveying bulk electric power across nations, so working to maintain the physical integrity of the transmission lines is an important goal. Each transmission line consists of a system of multiple towers, insulators, and conductors. Failures in the transmission system can lead to widespread power outages, which can impact other critical infrastructures such as natural gas, water, telecommunications, emergency services, and transportation [1,2].

Extreme weather is the major cause of transmission system disruptions [3]. It has been observed that the strong wind loads occurring from events such as hurricanes, tornadoes, and derechos are associated with approximately 80% of transmission tower failures in the Americas and Australia [4–6]. For example, in December 1982, high winds knocked over a 500 kV transmission tower, which then fell into a parallel 500 kV line tower, cutting power to more than 5 million people on the U.S. west coast. These initial failures caused a cascade of three further tower failures on each line [4]. During an inspection after Hurricane Michael in October 2018, it was observed that over 100 transmission towers toppled on the ground in a chain reaction like dominoes [7]. Other examples involving transmission line structural damage are Hurricane Sandy in 2012, which caused approximately 200 transmission line failures, and Hurricane Harvey in 2017, which caused damage to over 800 transmission line structures [8].

When a transmission tower has a structural failure, adjacent towers become more likely to fail because they are subject to unbalanced forces. The conductors on both sides of the tower have pretension forces that control the sag in each span, and when one of those forces is removed the tower has a large unbalanced force. The unbalanced force makes the adjacent towers more likely to fail, and if one of them does fail, its adjacent tower becomes more likely to fail. This progression of successive failures is cascading failure. The cascade failure can propagate until it stops by itself or until an anchor tower is reached. Anchor towers are built more strongly to withstand higher loads and the imbalanced forces caused by adjacent span failures [9,10]. A proper understanding of the anchor towers' role in limiting the cascade will help decide the placement of anchor towers.

This paper's topic of cascading structural failure of individual towers within a single transmission line has very limited previous work. Indeed the interdependencies between the parts of the transmission line are usually neglected. A few studies have analyzed the dynamic structural response of transmission tower parts under conductor breakage conditions. McClure et al. [11] used the finite element software ADINA to obtain the dynamic response of transmission line parts due to the

* Corresponding author.
E-mail address: alipour@iastate.edu (A. Alipour).

https://doi.org/10.1016/j.ress.2024.110304

Available online 28 June 2024

conductor breakage. Xue et al. 2020 [12] analyze in detail 3 towers, the conductors between the towers, and the interactions between the 3 towers and the conductors. Alminhana et al. [13] proposed a numerical modeling approach to calculate the dynamic response of transmission line parts triggered by conductor breakage. They developed a finite element model for a line of towers and used a lumped mass approach to solve uncoupled dynamic equilibrium equations and predict the tension force at the conductor insulator joint location. Their work was extended in their recent paper [14] where their numerical approach was used to conduct a deterministic structural cascade failure analysis for a finite element model of a line of eight towers under dynamic wind loads with broken conductors. The analysis considered two samples of time-dependent wind intensities and showed that structural cascading failure occurred during the sample with higher winds. To the best knowledge of the authors, [14] is the only other paper analyzing cascading structural failure of towers. Our approach differs from the deterministic finite element approach of [14] by using a fully probabilistic approach for analyzing structural cascade failures. Novel formulas for failure probabilities describing structural cascading are presented. The formulas can accommodate anchor towers in the line of towers and are scalable to apply to a larger number of towers in the line.

A transmission line is outaged (taken out of service so that it does not transmit power) by breakers at the ends of the line opening the circuit. Outages happen when there is an electrical fault on or near the line, when automatic or manual operations outage the line, or when there are structural failures in the line. This paper's topic of cascading structural failure of individual towers within a single transmission line can easily be distinguished from the topic describing the outage of transmission lines considered as a single entities under the stress of bad weather and by cascading outage of transmission lines caused by interactions within the electric network. Failure of a transmission line as a single entity does not address how individual tower failures interacted or how many towers failed; any number of towers failed will cause the entire line to outage. That is, cascading structural failure of towers addressed in this paper is a cascading process occurring within the transmission line between the parts of the transmission line.

There is extensive and wide ranging literature about transmission line outages with the transmission line considered as a single entity. For example, the resilience of entire transmission lines or an entire transmission network with respect to wind and other stresses (without any consideration of interactions between parts of the transmission line) is exemplified by [3,15–21] and the cascading of transmission line outages within the electric network is reviewed in [22–26]. Other authors similarly consider the outage of an entire transmission line and the network interactions between entire transmission lines, but determine the transmission outage using a fragility curve of single towers as in Mühlhofer et al. 2023 [27] or the fragility curve of each kilometer of line as in Scherb et al. 2019 [28]. However, in [27,28], the tower or line segment outages within the transmission line are assumed to be independent, so that there is no representation of a cascading effect *within* the transmission line.

This paper's new probabilistic approach to analyzing and quantifying the structural cascading of transmission towers within a transmission line starts by applying state of the art dynamic models of a tower–insulators–conductor system to obtain fragility curves describing the probability of structural failure as a function of wind loading. The fragility curves are combined with the distribution of annual maximum hurricane wind speeds to obtain an annual tower failure probability. This annual failure probability is calculated as p for a tower with intact adjacent towers and as q for a tower with damage to an adjacent tower. Now a line of transmission towers is considered, with a probability of initial tower failures p and a probability of further cascading tower failure of q if an adjacent tower failed. The probability distribution for the total number (initial plus cascading) of towers that failed is derived as a function of p and q using generating functions. The new formulas are generated and evaluated using computer algebra. The calculations allow for some of the towers to be anchor towers that do not fail. The probability distribution of the total number of towers failed enables the computation of the mean number of towers failed as a function of the anchor tower placement and also is combined with a cost analysis to give a life cycle cost that accounts for the additional towers failed due to cascading.

The principal contributions of the paper are summarized as follows:

1. The paper considers a line of general components that are subject to failure and derives new mathematical formulas to evaluate the probabilities of cascading failure extent, given the component failure probabilities when adjacent components are intact or failed.
2. The paper formulates the problem of structural cascading of transmission towers and gives the first probabilistic method to quantify the effects of this cascading by combining the new formulas with a detailed fragility analysis. The tower failure probabilities when adjacent towers are intact or failed are obtained with tower fragility curves based on a detailed state of the art dynamic analysis of transmission towers, insulators, and cables under straight line wind loads. An illustrative case study quantifies the effects of cascading and interspersed anchor towers in a line of twenty-five 500 kV towers.

Section 2 of the paper obtains the fragility curves and annual failure probabilities of a 500 kV tower design, and Section 3 derives the new formulas for the probability distribution of the number of towers failed and the mean number of towers failed in a line of towers. Section 4 estimates life cycle costs, which are combined with the probabilistic analysis in a case study illustrating the new approach in Section 5. Section 6 concludes the paper.

2. Fragility analysis for tower–conductor–insulator system

This section develops the fragility functions of a tower–insulator–conductor system with respect to wind speed and calculates its annual failure probabilities under straight line wind loads. The fragility functions build upon mechanistic models of the transmission tower–conductor–insulator system to assess the probability of failure for a system with intact adjacent towers and a system with a failed adjacent tower. Fragility functions are commonly described by the cumulative distribution function (CDF) of the two-parameter lognormal distribution as a function of the hazard intensity (wind speed, in this instance).

While the methodology has been used to some extent under other hazards such as earthquakes [29–36], only a few recent studies have been conducted on the fragility of specific power grid elements under straight line wind events. For example, Fu et al. [37] developed fragility curves for transmission towers subject to wind loading while considering the uncertainty of the wind only. Xue et al. [12] studied the transmission tower system outage and performance during a hurricane event by considering the physical impact of transmission tower-line interaction. Bi et al. [38] studied the wind-induced failure analysis of transmission tower systems based on field wind data and generated failure probabilities for these systems incorporating this data. Scherb et al. [28] assessed the importance of each part in a transmission tower system and evaluated the network performance for the Nordic grid by incorporating cascade failure utilizing a DC power flow model. Ma et al. [39] studied the impact of fragilities of transmission tower system parts under a hurricane by utilizing Monte Carlo simulation for failure probability calculation and further conducted a network analysis utilizing optimal power flow analysis. Teoh et al. [40] generated fragility curves for distribution poles under wind loadings for different pole decay rates and concluded with a life cycle cost analysis for each studied pole under wind loadings.

Due to the limited number of studies targeting the fragilities of transmission tower systems, there is a significant need to understand

Table 1
Material and geometric properties for tower, conductor, insulator.

	Transmission tower	
Material	A36 steel	
Dimensions	Cross sections based on structural drawing	
Young's Modulus	200 GPa	
Yield Stress	250 MPa	
	Conductor	Insulator
Outside diameter	0.025 m	0.34 m
Young's Modulus	65 GPa	100 GPa
Length	300 m	2.3 m
Density	2.67 kg/m	206.75 kg/m

the fragilities associated with each part of the tower system against wind events. The results from these fragilities can then be integrated into the formulas derived in Section 3 to quantify the cascading structural failure of towers probabilistically. The tower's experimentally validated finite element model was generated to achieve this goal. A stochastic wind model was developed to assess the likelihood of damage at different wind speeds utilizing dynamic analysis.

2.1. Finite element model for tower–insulator–conductor system

The finite element model for a single circuit 500 kV transmission tower system was created using ANSYS finite element modeling software. A beam truss model was adopted for the design, where the leg members of the tower were composed of beam members, and the primary bracing of the transmission tower was composed of truss members. Material and geometric nonlinearity was considered in the finite element models. The developed finite element model for the transmission tower was validated using the test-to-failure data provided by Bonneville Power Administration, which also provided the design details for the transmission tower.

The conductors and insulators were modeled with Link 180 elements that are ideal truss members and can only take tension or compression loads. The cables attached on the side of the tower are based on the catenary equation that considers span length, gravitational effects, and pretension in the cables. These cables or conductors are suspended through an insulator string on each side of the top part of the transmission tower. The length of the insulator string is 2.3 m with a mass of 8 kg. Table 1 summarizes the material and geometric properties of the tower, cables, and conductors comprising the transmission tower system.

A simplified single tower with attached conductors and insulator connections was modeled to increase computational efficiency. To capture the effect of adjacent spans, linear springs were added at the boundary conditions on each side of the adjacent spans of the tower to mimic the behavior of the additional spans. These springs accounted for the conductor's and the cross arm's stiffness from the adjacent towers. Fig. 1 shows the process of obtaining the simplified model of the transmission tower system. More details on creating the simplified tower system can be found in [41].

The failure modes considered in [41] were buckling and yielding of tower members for the transmission tower. For the conductors and insulators, exceedance of yield stress for the material was used as a failure mode. To account for the uncertainty arising from the structural properties, material uncertainty was introduced in the form of variation in Young's modulus and yield stress. The moment matching method was used to create finite element models statistically representing the variation in capacity [41]. Each of these models had its own limit states for each failure mode which were obtained employing nonlinear buckling analysis conducted in ANSYS. Dynamic wind loads were then applied to each of these models, and the resulting failure data for each uncertain model were combined to generate failure probability data that accounted for material uncertainty and wind load uncertainty. The system was considered to fail if one or more of the following conditions occurred: tower failure, conductors rupture, insulator assembly breakage.

2.2. Dynamic wind analysis for tower–conductor–insulator system

Dynamic wind loads were generated for the transmission tower system to account for the uncertainty from wind loads. Since the tower system has a significant vertical (tower height) and horizontal (conductor length) dimension, it was important to consider the impact of coherence of wind velocity fields along both these directions. Two different wind load models were used for generating the wind load time histories acting on the tower and the conductors. The wave superposition method [42,43] was used to handle the coherence between wind loads along the height of the transmission tower. The frequency wave number spectrum method [44] was used to handle the coherence along the cable span.

The mean wind loads were varied with wind speeds ranging from 0 m/s to 100 m/s. The simulation was repeated 100 times for each wind speed to capture the stochastic nature of wind loads. The wind loads/drag forces acting on each of the individual parts, including the tower, conductors, and insulators, were calculated using the following variation of the standard formula for drag force calculation:

$$F(z,t) = 0.5\rho C_D v(z,t)^2 A \tag{1}$$

where A is the projected area perpendicular to wind direction flow, C_D is the drag coefficient for each of the parts, i.e., the tower, insulators, and conductors, ρ is the air density, and $v(z,t)$ are the time history of velocities that are generated for the tower, conductors and insulators respectively as a function of time and height.

Wind tunnel studies were conducted to determine the drag coefficients for the tower by separating the tower into three segments: the bottom section (legs), the middle part, and the top part. This allowed for the generation of realistic drag forces for the tower for various orientations. Alipour et al. [45] provides more details on the method used to determine the drag coefficients for various tower orientations. The computation of drag forces operating on the conductors used realistic drag coefficients for conductors based on work by Jafari and Sarkar [46] for various wind directions. More details on how the dynamic loads were applied to the system can be found in [41].

2.3. Fragility estimation for tower–insulator–conductor system

The maximum likelihood approach was used to fit obtained failure probability values to the lognormal distribution form of the fragility curves in the literature [12,37]. More information about this approach can be found in [41].

The fragility curves were established for two different states of the system: intact and damaged. The intact system had no damage, and the damaged system had ruptured conductors. It should be noted that the damaged system did not include explicit dynamic analysis representing the impact load from the conductor breakage. It, however, represented unbalanced loads (after sudden rupture) on the transmission tower, resulting in a higher probability of failure for the damaged system than the intact system. The assumption made here for the damaged system is that the tower has survived the initial impact load because of conductor breakage and the results shown are for fragility curves for an intact tower–conductor and broken conductor–tower systems modeled using the ANSYS element birth death approach. The generated fragility curve for the transmission tower system for both the cases under the limit state of buckling is shown below in Fig. 2(a) for the case where the wind direction is perpendicular to the transmission line. Fig. 2(b) shows the wind direction with respect to the tower orientation at a general angle α. The probability of failure observed for the intact system is lower than that of the damaged system.

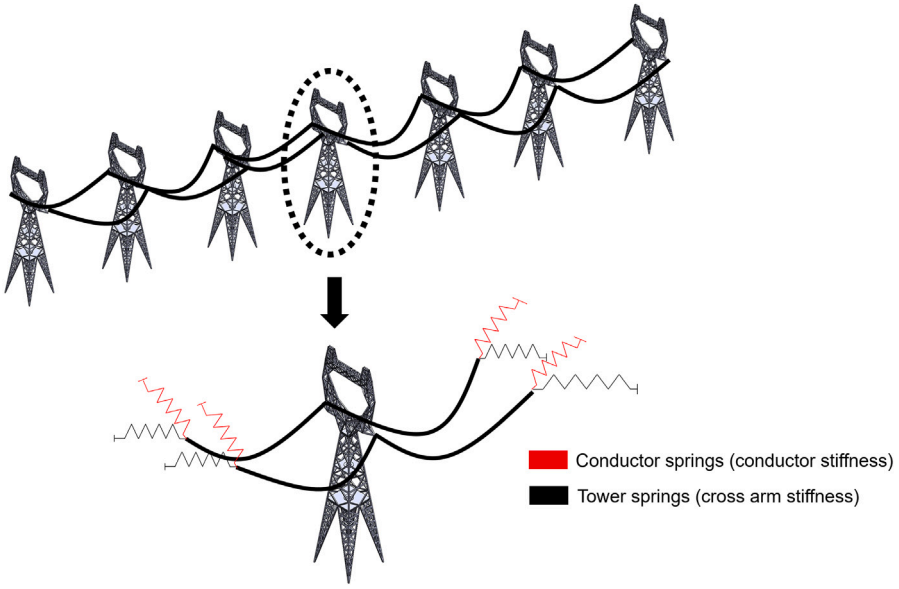

Fig. 1. Configuration of the tower–conductor system and the springs representing the boundary conditions.

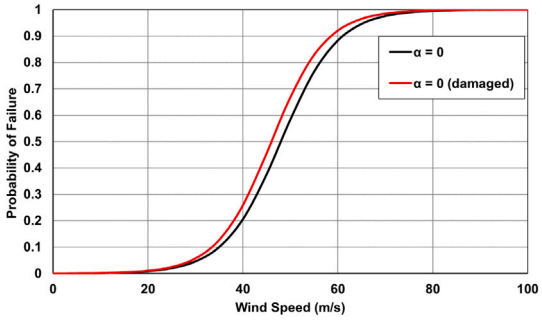

(a) Fragility for intact and damaged system for line perpendicular to wind flow ($\alpha = 0$).

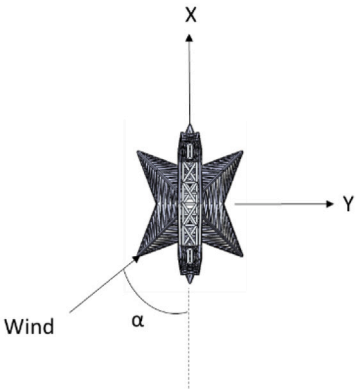

(b) Tower orientation with respect to wind direction, highlighting angle α.

Fig. 2. Fragility curves for intact and damaged system.

The probability of tower failure also depends on the direction of the incoming wind with respect to the transmission line alignment. To account for this effect, the wind angle of attack was varied from 0–90° with 15° increments. The wind direction impacts the fragility functions for two reasons: (1) with the changing wind direction, the exposed surface of the conductor and tower to wind changes, which results in a change in wind pressure, and (2) for every tower orientation, there exists a different value of limit state after which failure is observed (see Fig. 3 for the tower tip displacement in meters). Fig. 4 shows the fragility functions of intact and damaged towers for different wind directions.

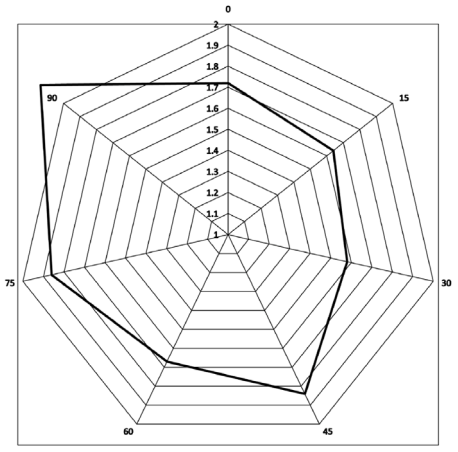

Fig. 3. Rose diagram for transmission tower limit states.

2.4. Calculating the annual probability of failure from the wind hazard

To obtain the annual failure probability for the tower–insulator–conductor system, it is important to consider the probability of the wind hazard together with the fragility curves discussed in Section 2.3. For this purpose, the probability of failure for different wind speeds is extracted from the fragility curves for both intact and damaged cases and combined with the maximum wind speed probability distribution.

Wind speed data for Miami Beach, FL was used as a representative of one of the most vulnerable places for hurricanes. Yeo et al. [47] observed that an extreme value distribution (reverse Weibull) function was a good fit for simulated annual maximum hurricane wind speed

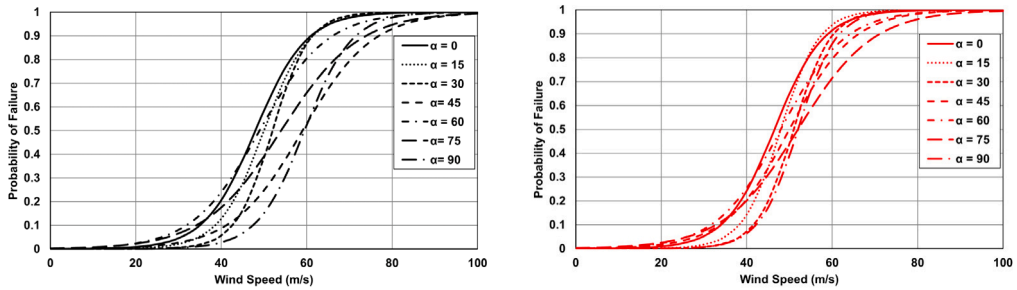

(a) Intact system (b) Damaged system

Fig. 4. Fragility curves for transmission tower system for different wind directions.

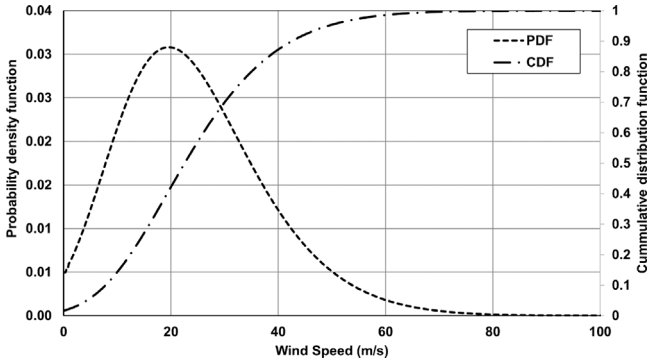

Fig. 5. Wind speed reverse Weibull distribution for Miami Beach, FL.

data, including Miami Beach. The annual probability of maximum wind speed U being less than a specified value v is the wind cumulative distribution function $H_U(v)$, which for the reverse Weibull distribution is

$$H_U(v) = P(U \le v) = \exp\left[-\left(\frac{b-v}{a}\right)^{\frac{-1}{c}}\right], \quad v \le b \tag{2}$$

where U is the annual maximum hurricane wind speed, v is the hurricane wind speed (m/s), a is the scale parameter, b is the location parameter, and c is the tail length parameter. The fitted values of a, b, and c for Miami Beach, FL from [47] are 123.70, 141.96 m/s and –0.097 respectively. The distribution of U is shown in Fig. 5.

The probability of failure $P(F|U = v)$ for wind speed U equal to v is obtained from the fragility curves for the intact or damaged systems developed in Fig. 4. The annual probability of tower failure P_a is then the fragility for a given wind speed weighted by the wind probability density function $\frac{dH_U(v)}{dv}$ integrated over all wind speeds:

$$P_a = \int_0^\infty P(F|U = v)\frac{dH_U(v)}{dv}\,dv \tag{3}$$

The annual failure probability, Eq. (3) can be evaluated for either intact or damaged systems by using the corresponding fragility curves in Fig. 4 to obtain $P(F|U = v)$.

3. Deriving cascading failure probabilities in a line of towers

This section calculates the probabilities of the number of failed towers in a line of transmission towers accounting for the cascading by which the initial tower failures propagate to further tower failures. The analysis applies generally to any line of general components subject to initial failure and cascading failure along the line, but here it is convenient to explain the analysis in terms of its application to transmission towers, referring to the components as towers.

It is assumed that N towers are in the line between two anchor towers. The anchor towers are assumed not to fail. It is a well-known fact that estimating horizontal coherence across tower spans becomes increasingly challenging, particularly with expanding separation distances [44,48]. Also, the coherence values significantly go down in magnitude as the separation distance increases. Consequently, in examining the cascade along the line, the authors opted to assume that wind speeds at different tower locations are independent of one another. Thus, the towers are subject to wind loads assumed to be the same for each tower and constant over time. The failures are divided into initial failures of towers followed by cascading failures of towers that had an adjacent tower fail. The initial tower failures are simultaneous and independent with probability p. Once the initial towers fail, more towers fail in succession in a cascade because they are adjacent to failed towers until that cascade of failures stops. We model the order but not the timing of the cascading after the initial failures. Multiple cascades in the line of towers separated by an intact tower are assumed to be independent processes. A tower has a probability q of failing if an adjacent tower has failed. When applying the formulas derived in this section, the values of p and q are obtained from Eq. (3) for the intact and damaged systems, respectively.

3.1. Initial tower failures

This subsection computes the probability of the initial failures in the straight line of transmission towers. The initial failures of the N towers are independent and have probability p. Let

$$S_r = \mathrm{I}[\text{tower } r \text{ initially fails}], \quad r = 1, 2, \ldots, N, \tag{4}$$

where I is the indicator function. Then $S_1, S_2, \ldots, S_N$ are i.i.d. Bernoulli with $\mathrm{P}[S_1 = 1] = p$. Let S be the number of initial tower failures

$$S = S_1 + S_2 + \cdots + S_N. \tag{5}$$

Let Π_S be the set of permutations of S initially failed towers and $N - S$ initially intact towers. An initially failed tower is represented as a one and an initially intact tower is represented as a zero so that each permutation is represented as a row vector of S ones and $N - S$ zeros. Let $\pi_1 \in \Pi_S$ be one of the permutations. We have

$$\mathrm{P}[(S_1, S_2, \ldots, S_N) = \pi_1] = p^S(1-p)^{N-S} \tag{6}$$

3.2. Blocks of initially intact towers that undergo cascading failure

The pattern of the S initially failed towers causes there to be blocks of initially intact towers between the anchor towers and the next initially failed tower (which we call "a blocks"), and between any two successive initially failed towers (which we call "b blocks"). Fig. 6 shows an illustration for how the a and b blocks are defined for a line of regular towers separated by two anchor towers at each end.

The a and b blocks of initially intact towers are both subject to cascading failure. The a blocks can cascade from the failed tower at

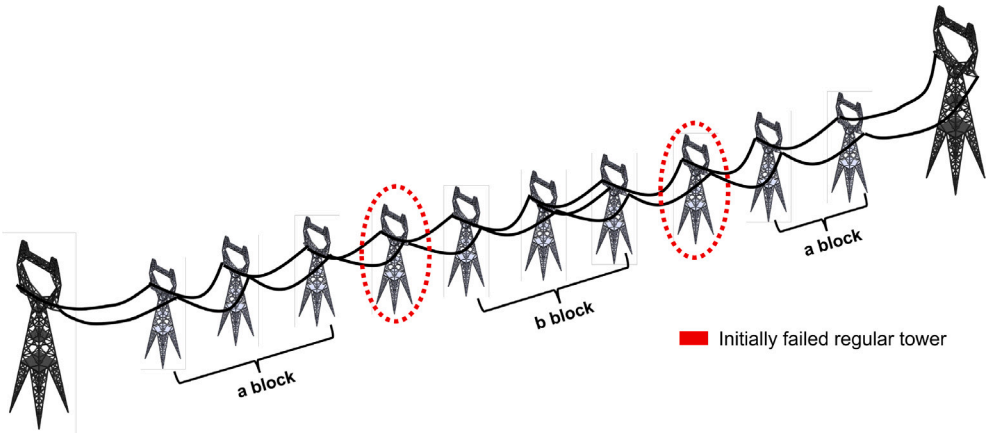

Fig. 6. Example showing initially failed towers circled in red and a and b blocks of towers. The anchor towers are schematically shown larger; they are built stronger and can have a different form.

one end towards the anchor tower, and the b blocks can cascade from both ends.

The number of towers failing in a cascade in a block depends on the length (number of towers) M of the block. Let the number of towers failing by cascading in an a block be $T_a(M)$ and the number of towers failing by cascading in a b block be $T_b(M)$. Let the generating functions of $T_a(M)$ and $T_b(M)$ be $G_{T_a}(z, M)$ and $G_{T_b}(z, M)$ respectively. The computation of $G_{T_a}(z, M)$ and $G_{T_b}(z, M)$ is postponed to Section 3.3.

Each permutation $\pi \in \Pi_S$ has S towers initially failed and therefore $S+1$ blocks of intact towers. Let $B_1(\pi), B_2(\pi), \ldots, B_{S+1}(\pi)$ be the block lengths for permutation $\pi \in \Pi_S$. Some of the blocks may be empty; this happens when the tower next to an anchor tower initially fails, or when two adjacent towers initially fail. Empty blocks have length zero. The total number of initially failed and cascaded towers for permutation $\pi \in \Pi_S$ is

$$T_\pi = \begin{cases} 0 & , S = 0 \\ 1 + T_a(B_1(\pi)) + T_a(B_2(\pi)) & , S = 1 \\ S + T_a(B_1(\pi)) + \left[\sum_{i=2}^{S} T_b(B_i(\pi))\right] + T_a(B_{S+1}(\pi)) & , S \geq 2 \end{cases} \tag{7}$$

Since the cascades in each block are independent, and the initial failures are independent of the cascading, the generating function of T_π is

$$G_{T_\pi}(z) = \begin{cases} 1 & , S = 0 \\ z\, G_{T_a}(z, B_1(\pi))\, G_{T_a}(z, B_2(\pi)) & , S = 1 \\ z^S G_{T_a}(z, B_1(\pi)) \left[\prod_{i=2}^{S} G_{T_b}(z, B_i(\pi))\right] G_{T_a}(z, B_{S+1}(\pi)) & , S \geq 2 \end{cases} \tag{8}$$

Let T be the total number of failed towers.

$$\begin{aligned} \mathrm{P}[T = r] &= \sum_{S=0}^{N} \sum_{\pi \in \Pi_S} \mathrm{P}[\pi]\, \mathrm{P}[T = r|\pi] \\ &= \sum_{S=0}^{N} p^S (1-p)^{N-S} \sum_{\pi \in \Pi_S} \mathrm{P}[T_\pi = r] \end{aligned} \tag{9}$$

The generating function of the total number of failed towers T is

$$G_T(z, N) = \sum_{S=0}^{N} p^S (1-p)^{N-S} \sum_{\pi \in \Pi_S} G_{T_\pi}(z) \tag{10}$$

In Eq. (10), the generating function variable is z. The mean total number of towers failed is then the derivative of the generating function evaluated at one:

$$\mathrm{E}T(N) = G'_T(1, N) \tag{11}$$

3.3. Cascading in the initially intact blocks of towers

This subsection computes the probability generating functions for the cascade failures occurring in the a and b blocks. That is, we now calculate the generating functions $G_{T_a}(z, M)$ and $G_{T_b}(z, M)$ to find the distribution of the number of cascading failures in each block of towers that is intact after the initial failures.

The a blocks can only cascade from one end of the block. Recall that the number of intact towers in a block is M. Then

$$P[T_a = r] = \begin{cases} q^r(1-q) & , r = 0, 1, \ldots, M-1 \\ q^M & , r = M \end{cases} \tag{12}$$

and the generating function is

$$\begin{aligned} G_{T_a}(z, M) = \mathrm{E}z^{T_a} &= \Big[\sum_{r=0}^{M-1} (qz)^r (1-q)\Big] + (qz)^M \\ &= (1-q)\frac{1-(qz)^M}{1-qz} + (qz)^M \end{aligned} \tag{13}$$

The b blocks can cascade from both ends of the block. Let R_1 be the number of towers failing from one end of the block and R_2 be the number of towers failing from the other end. Then $T_b = R_1 + R_2$ and $0 \leq T_b \leq M$.

Suppose that $M \geq 1$ and $T_b < M$. Then the two cascades are independent and

$$\mathrm{P}[R_1 = r_1] = q^{r_1}(1-q) \tag{14}$$

$$\mathrm{P}[R_2 = r_2] = q^{r_2}(1-q) \tag{15}$$

$$\mathrm{P}[R_1 = r_1 \text{ and } R_2 = r_2] = q^{r_1+r_2}(1-q)^2 \tag{16}$$

$$\mathrm{P}[T_b = r] = \mathrm{P}\Big[\bigcup_{r_1=0}^{r} \{R_1 = r_1 \text{ and } R_2 = r - r_1\}\Big] \tag{17}$$

$$= \sum_{r_1=0}^{r} \mathrm{P}[R_1 = r_1 \text{ and } R_2 = r - r_1] \tag{18}$$

$$= (r+1)q^r(1-q)^2, \quad r = 0, 1, 2, \ldots, M-1 \tag{19}$$

Also

$$\begin{aligned} \mathrm{P}[T_b = M] &= 1 - \mathrm{P}[T_b < M] \\ &= 1 - \sum_{r=0}^{M-1} (r+1)q^r(1-q)^2 \\ &= q^M(M + 1 - Mq) \end{aligned} \tag{20}$$

From Eqs. (19) and (20) the generating function for $M \geq 1$ is

$$G_{T_b}(z, M) = Ez^{T_b}$$

$$= \Big[\sum_{r=0}^{M-1}(r+1)(qz)^r(1-q)^2\Big] + (qz)^M(M+1-Mq)$$
$$= \frac{(1-q)^2}{(1-qz)^2}\left[1-(M+1-Mqz)(qz)^M\right] + (qz)^M(M+1-Mq) \quad (21)$$

Moreover, if $M = 0$, then $\mathrm{P}[T_b = 0] = 1$ and $G_{T_b}(z,0) = 1$, so that Eq. (21) is valid for all $M \geq 0$.

3.4. Formula evaluation via computer algebra

This subsection combines and evaluates the formulas Eqs. (10), (8), (13), (21) of the previous subsections to obtain the generating function of the number of failed towers as a function of the number of towers N between the anchor towers. This important step is challenging to do by hand, because enumerating and evaluating all the permutations of the blocks of initially intact towers is onerous. However, the formulas are quite readily evaluated by means of computer algebra. For example, for $N = 3$, we use Mathematica to compute

$$\begin{aligned} G_T(z,3) &= (1-p)^3 \\ &+ z\left(p(p-1)^2q^2 - 4p(p-1)^2q + 3p(p-1)^2\right) \\ &+ z^2\left((1-p)p^2q^2 + 4p^2(p-1)q - 3p^2(p-1) - 4p(p-1)^2q^2 + 4p(p-1)^2q\right) \\ &+ z^3\left(p^3 + (p-1)p^2q^2 - 4(p-1)p^2q + 3(p-1)^2pq^2\right) \end{aligned} \quad (22)$$

The formula complexity and the necessity for computer algebra increase rapidly with N. For example, Mathematica computes the formula for $N = 5$ as

$$\begin{aligned} G_T(z,5) &= (1-p)^5 \\ &+ z[3p(p-1)^4q^2 - 8p(p-1)^4q + 5p(p-1)^4] \\ &+ z^2[-p^2(p-1)^3q^4 + 8p^2(p-1)^3q^3 - 21p^2(p-1)^3q^2 + 24p^2(p-1)^3q \\ &\quad - 10p^2(p-1)^3 + 4p(p-1)^4q^3 - 12p(p-1)^4q^2 + 8p(p-1)^4q] \\ &+ z^3[p^3(p-1)^2q^4 - 8p^3(p-1)^2q^3 + 21p^3(p-1)^2q^2 - 24p^3(p-1)^2q \\ &\quad + 10p^3(p-1)^2 + 9p^2(p-1)^3q^4 - 36p^2(p-1)^3q^3 + 51p^2(p-1)^3q^2 \\ &\quad - 24p^2(p-1)^3q + 3p(p-1)^4q^4 - 12p(p-1)^4q^3 + 9p(p-1)^4q^2] \\ &+ z^4[-3p^4(p-1)q^2 + 8p^4(p-1)q - 5p^4(p-1) - 2p^3(p-1)^2q^4 \\ &\quad + 20p^3(p-1)^2q^3 - 42p^3(p-1)^2q^2 + 24p^3(p-1)^2q - 18p^2(p-1)^3q^4 \\ &\quad + 48p^2(p-1)^3q^3 - 30p^2(p-1)^3q^2 - 8p(p-1)^4q^4 + 8p(p-1)^4q^3] \\ &+ z^5[p^5 + 3(p-1)p^4q^2 - 8(p-1)p^4q + (p-1)^2p^3q^4 - 12(p-1)^2p^3q^3 \\ &\quad + 21(p-1)^2p^3q^2 + 10(p-1)^3p^2q^4 - 20(p-1)^3p^2q^3 + 5(p-1)^4pq^4] \end{aligned} \quad (23)$$

3.5. Cascading probabilities in a line of towers with multiple anchors

The calculations can be extended to a line of towers with multiple sections separated by A anchor towers. The two end towers are anchor towers and there are $A-2$ anchor towers in between separating $A-1$ sections of regular towers. Suppose that section i has N_i towers. Then the total number of all towers is $L = A + N_1 + N_2 + \cdots + N_{A-1}$. We write F for the total number of towers failed in all the sections. Since the failures in the sections are independent, the generating function of F is

$$G_F(z, N_1, N_2, \ldots, N_{A-1}, A) = \prod_{i=1}^{A-1} G_T(z, N_i) \quad (24)$$

If the anchor towers are equally spaced so that the number of regular towers is N in each section, then $N = (L-A)/(A-1)$. Hence $A = (L+N)/(N+1)$, the number of sections is $A-1 = (L-1)/(N+1)$, and (24) becomes

$$G_F(z, N, L) = (G_T(z,N))^{A-1} = (G_T(z,N))^{\frac{L-1}{N+1}} \quad (25)$$

Table 2
Cost parameters and their values for life cycle cost analysis.

Parameter	Value	Description [reference]
r	4% per year	Discount rate
C_{CR}	\$190,474	Construction (regular tower) [49]
C_{CA}	\$594,779	Construction (anchor tower) [49]
	50 years	Tower lifetime [40,50]
n	9	Number of inspections
Δt	5 years	Inspection interval
$S+M$	\$20,000	Inspection and maintenance [51]
C_{remove}	\$59,806	Tower removal [49]
C_R	\$250,279	Tower replacement [49]
$C_{customer}$	\$840,000 per hour	Customer outage [52]
t_{repair}	40 h	Time to repair [41,53]
f_{ENS}	20%	Probability of customer outage

The probability of k towers failed $p_k(N)$ can be easily extracted from the generating function Eq. (24) or, in the equally spaced case, Eq. (25). Moreover, the mean total number of towers that failed is given in general by

$$\overline{F} = G'_F(1, N_1, N_2, \ldots, N_{A-1}, A) = \sum_{j=1}^{A-1} G'_T(1, N_j) \quad (26)$$

or in the equally spaced case,

$$\overline{F} = G'_F(1, N, L) = (A-1)G'_T(1, N) = (A-1)G'_T\left(1, \tfrac{L-A}{A-1}\right) \quad (27)$$

These formulas incorporating probability generating functions can be generated and evaluated with computer algebra to calculate the failure probabilities for initial structural failures of transmission towers and subsequent cascade failures of these towers under a given straight line wind event. In particular, the probability generating functions can be used to generate the failure probabilities for different configurations of anchor towers in a line of transmission towers.

4. Life cycle cost analysis for transmission towers

The life cycle cost includes the major costs of the transmission line from the beginning of construction planning to the end of the service life. The life cycle cost is a necessary part of the analysis to choose the most cost-effective design of tower–anchor tower arrangements. The life cycle cost is calculated from the present value of the construction cost, inspection and maintenance costs, failure costs, and customer outage costs. This section reviews these costs and their assumptions. All the parameter values used in the cost calculations are given in Table 2.

The different components of the life cycle cost of a line of L towers with A anchor towers are

$$LCC = AC_{CA} + (L-A)C_{CR} + L(C_{IN} + C_M) + C_{wf(line)} + C^{cust}_{wf(line)} \quad (28)$$

where LCC stands for life cycle cost, C_{CR} is the initial construction cost of a regular tower, C_{CA} is the initial construction cost of an anchor tower, C_{IN} is the inspection cost, C_M is the maintenance cost, C_{wf} is the transmission tower failure cost, and C^{cust}_{wf} is the customer cost associated with transmission line failure. The initial construction, inspection, and maintenance costs are incurred regardless of any failures. Here we are particularly interested in the failure and customer costs that depend on tower failure due to wind and are affected by cascading.

Since inspection, maintenance, and failure happen at different times, inflation and opportunity costs significantly affect the present value of these costs. For the present value life cycle cost analysis, these recurrent costs are combined by weighting them at year t using the discount factor

$$z(t) = (1+r)^{-t} \quad (29)$$

where the discount rate r reflects the expected market rate of return on investment and usually varies from 2% to 8% in practice. We use $r = 4\%$ per year.

4.1. Initial construction cost

The initial cost of tower construction assumes a 500 kV AC straight line of steel towers. The construction costs for a regular (tangent) tower C_{CR} and an anchor (dead-end) tower C_{CA} are obtained from the Midcontinent Independent System Operator (MISO) database [49]. The obtained values of C_{CR} and C_{CA} are \$190,474 and \$594,779 respectively. These values include the cost of materials, installation, hardware, and foundation for both regular and anchor towers.

4.2. Maintenance and inspection costs

The costs of inspection and maintenance are expected to be incurred at regular time intervals, Δt, and can be calculated as:

$$C_{IN} + C_M = \sum_{i=1}^{n} (S + M) z(i\Delta t) \tag{30}$$

where S is the cost of each inspection, and M is the cost of maintenance activities in base year prices. $S + M$ = \$20,000 for both regular and anchor towers based on [51]. We assume that transmission towers are inspected every Δt = 5 years, based on information available online [54]. We assume a transmission tower lifetime of 50 years [40,50]. Thus there are n = 9 inspections during the life of the transmission tower. The failure cost includes performing the inspection and repairing a damaged tower. It is assumed that regardless of the inspected wear and tear, the maintenance cost is fixed, and the tower is restored to its pristine condition each time. Vegetation management and wildlife protection costs are not included due to the limited availability of that information. We do not include any customer costs for maintenance, since maintenance is usually planned and executed to avoid any customer interruption.

4.3. Direct failure costs for a tower and a line of towers

Failure costs include direct costs (for repair and replacement) and indirect costs (for customer losses). Only failure due to high wind is considered here.

Consider the replacement cost C_R of a single failed regular tower. The failed tower is considered irreparable, so that a new tower is required. Therefore the replacement cost is the removal cost plus the initial construction cost C_{CR}. The removal cost C_{remove} = \$59,806 for a 500 kV tower is estimated from [49], and $C_R = C_{CR} + C_{remove}$ = \$250,279.

The calculated value of C_R can be used to evaluate the cost of multiple tower failures in a line of towers. The mean number of towers failed in each year $\overline{F}$ is obtained from Eq. (27). Then the mean failure cost for a line of towers over its lifetime of 50 years is

$$C_{wf(line)} = \sum_{t=0}^{49} C_R \overline{F} z(t) \tag{31}$$

4.4. Customer costs due to failures in a line of towers

In addition to the failure cost, which is directly related to the repair and replacement costs of the transmission line components, the customers have costs (losses) from the power outages that can result from the failure. The main portion of transmission grids are designed with redundancy as a meshed network with parallel paths to supply a given distribution substation. Failures in a single transmission line that is in the meshed portion of the grid often result in a manageable redistribution of grid flows so that the distribution system remains energized and there are no customer outages. However, there are cases in which transmission line failure causes a blackout, when it causes severe unbalanced flows or transients, or when multiple transmission lines fail. One example is Hurricane Ida, in which more than a million customers were left without power, mostly due to one transmission tower failure [55]. Here we study a 500 kV transmission line that carries large bulk power flows and it is correspondingly impactful when it fails. Another complication is that extreme winds often can also extensively damage the lower voltage distribution system. The customer power requires both the transmission and distribution system to be repaired and restored. The transmission line repair has a high priority due to its high impact, but the delay in restoring customer's power can have contributions from the delays in restoring both the transmission system and the distribution system. All these considerations make the link between failure of a single transmission line and customer power outages plausible in some cases but considerably uncertain. We represent this link by a probability $f_{\mathrm{ENS}} = 20\%$ that the transmission line failure impacts the customer power.

Now we address the customer costs due to power outage. These costs depend heavily on industrial and commercial customers and are not well known for the longer duration outages of most interest. We use a rough order of magnitude estimate for the hourly incurred customer costs $C_{customer}$ = \$840,000 per hour [52] by converting to US dollars and accounting for inflation.

One tower takes a mean time of t_{repair} hours to repair. We roughly estimate t_{repair} by taking a weighted mean of the repair times for the tower, conductors, and insulators. The assumed mean values of repair times for the tower, insulators, and conductors are t_{repair}^{tower} = 150 h, $t_{repair}^{conductor}$ = 10 h, and $t_{repair}^{insulator}$ = 5 h [53]. The failure probabilities for these components are P_{tower}^{f} = 0.22, $P_{conductor}^{f}$ = 0.66, and $P_{insulator}^{f}$ = 0.33 [41]. Then the mean time of repair is

$$t_{repair} = P_{tower}^{f} t_{repair}^{tower} + P_{conductor}^{f} t_{repair}^{conductor} + P_{insulator}^{f} t_{repair}^{insulator} = 40 \text{ h} \tag{32}$$

The assumed value of $C_{customer}$ and t_{repair} can further be used to evaluate the cost of multiple tower failures in a line of towers. According to [52], for $F \geq 1$ failed towers in a line of N regular towers the mean repair time is $t_{repair} H(F)$, where

$$H(F) = \sum_{i=1}^{F} \frac{1}{i} \tag{33}$$

is the harmonic number function [56]. $H(F)$ always increases as the number of failed towers F increases, but it increases more slowly for additional failed towers since it is more efficient to repair an additional tower because the crews, equipment, materials, and temporary structures are all in place. Limited literature is available on the time to repair transmission towers, but the harmonic number dependence has been qualitatively checked as consistent with engineering experience [52].

Then the mean repair time for a line of cascading towers is

$$t_{repair(line)} = t_{repair} H(F) = t_{repair} \sum_{f=1}^{N} P[F = f] H(f) \tag{34}$$

Finally, the expected value of customer costs in a line of cascading towers is

$$C_{wf(line)}^{cust} = \sum_{t=0}^{49} C_{customer} t_{repair(line)} f_{\mathrm{ENS}} z(t) \tag{35}$$

We acknowledge that Eq. (35) is a very rough estimate, in large part because of the large uncertainty in the estimates of the fraction f_{ENS} of transmission line outage directly impacting the customers and the hourly customer costs $C_{customer}$. However, unless there is an exclusive focus only on costs directly borne by the utility, even a very rough estimate coupled with suitable attention to the consequent large uncertainty in the results is better than neglecting the customer costs entirely. We emphasize the importance of future work relating transmission line outages to customer impact. One approach uses symbolic regression on simulated outages to obtain formulas for energy not served in terms of the line voltage rating, the repair time, and the outage month [57].

Table 3
A and N in a line of 25 towers.

Number of anchor towers A	2	3	4	5	6	7	8	9
Average number N of towers in section	23	11	7	5	3.8	3	2.43	2

5. Design example of a line of twenty-five towers

The design example considers failures in a line of twenty-five 500 kV towers with and without cascading, and with and without customer costs. The effects of cascading failure and the number of anchor towers are quantified and the corresponding life cycle costs are obtained.

5.1. Cascading failure and cost calculations in a line of towers

The design example considers a straight line of $L = 25$ towers. There are A anchor towers, including the two anchor towers at each end. The anchor towers are designed with more strength and are assumed not to fail. Since the results of Fig. 4 show that the wind acting perpendicular to the line causes the highest probability of failure in the tower, this assumption is used to assess the highest annual probability of failure of the line system. For the regular towers, the fragility curves corresponding to tower orientation of 0° for the intact and damaged cases shown in Figs. 4(a) and 4(b) are used. The two fragility curves are first combined with the hazard curve using Eq. (3) to obtain the annual failure probabilities $p = 0.08$ for an intact tower and $q = 0.15$ for a damaged tower. Similarly, the fragility curve for any given angle of attack can be extracted from Fig. 4 and its product taken with the wind speed probability distribution presented in Fig. 5 to obtain the annual probability of failure of the tower system for that wind angle of attack.

Given the values of p, q, A and L, the distribution of the number of tower failures is calculated from Section 3 using Eqs. (24) and (25), and the mean number of towers failed is calculated using Eq. (27). Then the life cycle cost is calculated from Section 4 using Eq. (28). This calculates the case with cascading and with customer costs. The cases with no cascading are easily obtained by setting $q = 0$ so that only initial failures are considered, and the cases with no customer costs are easily obtained by setting $C^{cust}_{wf(line)} = 0$.

In this design example, we evaluate the statistics of cascading tower failure and evaluate the cost as the number of anchor towers varies. The A anchor towers are chosen to be equally spaced or equally spaced as nearly as possible. There are $A - 1$ sections of towers between anchor towers, and each section has average number of towers N as shown in Table 3. Some numbers of anchor towers divide the towers equally. For example, if there are 4 anchor towers, these anchor towers separate the rest into 3 equal sections with 7 towers each. Some other numbers of anchor towers divide the towers only nearly equally. For example, if there are 6 anchor towers, then these anchor towers separate the rest of the towers into 4 sections with 4 towers each and one section with 3 towers.

5.2. Results for the probability distribution of number of towers

Fig. 7 shows the probability distribution of the number of failed towers as the number of anchor towers A varies when cascading is considered. Increasing the number of anchor towers shifts the probability distribution towards a smaller number of towers and decreases the probability of large cascades for two reasons: (1) Any cascade of failures reaching an anchor tower stops because the anchor tower does not fail, thus limiting the cascade spread; (2) An increased fraction of anchor towers limits the initial tower failures.

Fig. 8 shows the probability distribution of the number of failed towers as the number of anchor towers A varies without considering cascade failures. Increasing the number of anchor towers shifts the probability distribution towards a smaller number of towers because an increased fraction of invulnerable anchor towers limits the number of initial tower failures. However, this effect is smaller than when cascading is considered, as can be seen by comparing the shifts in the probability distributions in Figs. 7 and 8. The main effect of including cascading is that it significantly shifts the probability distributions towards larger cascades, increasing the probability of large cascades and decreasing the probability of small cascades.

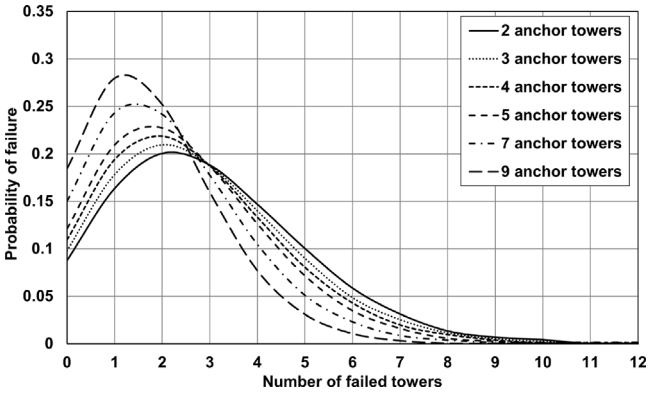

Fig. 7. Probability distribution of the number of tower failures for a line of 25 towers with cascading.

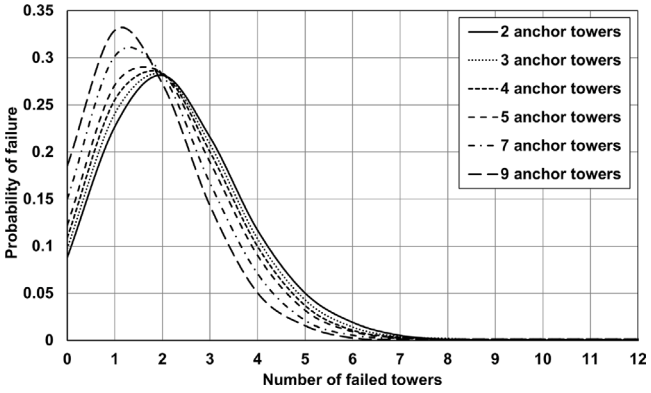

Fig. 8. Probability distribution of the number of tower failures for a line of 25 towers with no cascading.

Fig. 9 shows how the mean number of tower failures decreases as the number of anchor towers increases, both with and without cascading. When cascading is considered, the mean number of towers failed increases by 0.6 towers for two anchor towers. The amount of this increase is less as the number of anchor towers increases because the anchor towers limit the extent of the cascades and thus limit the effect of considering cascading.

5.3. Results for life cycle cost for a line of 25 towers

The breakdown of the life cycle cost of the line of 25 towers with and without cascading and customer cost is shown in Table 4. For all the different cases, it can be seen that the initial cost of construction goes up as the number of anchor towers is increased, but the cost of failure and the customer cost due to failure goes down. This is expected because the anchor towers are more expensive and are assumed not to fail.

The total life cycle costs for the different cases are shown in Table 4 and also plotted in Fig. 10. Consider first the cases that neglect customer cost as shown in Fig. 11. The life cycle cost slowly decreases as the number of anchor towers increases. As the number of anchor towers increases from 2 to 9, the life cycle cost decreases by 13% with

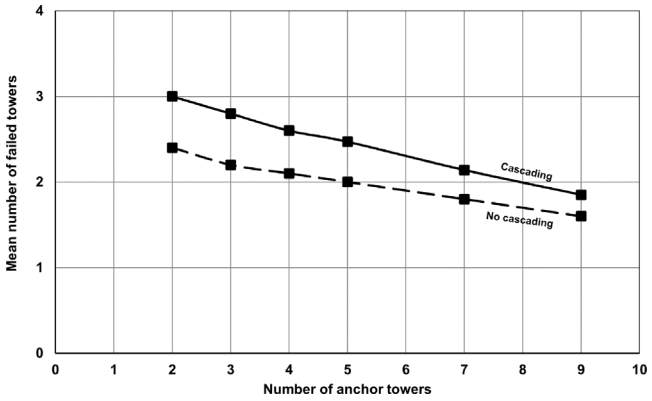

Fig. 9. Mean number of towers failed.

Table 4
Life cycle costs in a line of 25 transmission towers for different numbers of anchor towers considering the effects of cascade and customer cost.

# anchor towers	Cascading					
	2	3	4	5	7	9
C_C	5570	5975	6379	6783	7592	8401
$C_{IN}+C_M$	1913	1913	1913	1913	1913	1913
C_{wf}	16 774	15 655	14 537	13 978	12 301	10 847
$C^{cust}_{wf(line)}$	246 205	237 197	234 195	222 185	208 673	183 152
LCC_{line}	24 256	23 542	22 829	22 674	21 805	21 160
	No cascading					
C_C	5570	5975	6379	6783	7592	8401
$C_{IN}+C_M$	1913	1913	1913	1913	1913	1913
$C_{wf(line)}$	13 419	12 301	11 742	11 182	10 064	8946
$C^{cust}_{wf(line)}$	223 147	215 842	208 702	205 251	193 831	179 151
LCC_{line}	20 902	20 188	20 033	19 878	19 568	19 259
	Cascading and Customer cost					
C_C	5570	5975	6379	6783	7592	8401
$C_{IN}+C_M$	1913	1913	1913	1913	1913	1913
$C_{wf(line)}$	16 774	15 655	14 537	13 978	12 301	10 847
$C^{cust}_{wf(line)}$	246 205	237 197	234 195	222 185	208 673	183 152
LCC_{line}	270 462	260 740	257 024	244 859	230 479	204 313
	No cascading and Customer cost					
C_C	5570	5975	6379	6783	7592	8401
$C_{IN}+C_M$	1913	1913	1913	1913	1913	1913
$C_{wf(line)}$	13 419	12 301	11 742	11 182	10 064	8946
$C^{cust}_{wf(line)}$	223 147	215 842	208 702	205 251	193 831	179 151
LCC_{line}	244 049	236 030	228 735	225 130	213 400	198 410
	Cascading and Reduced customer cost					
C_C	5570	5975	6379	6783	7592	8401
$C_{IN}+C_M$	1913	1913	1913	1913	1913	1913
$C_{wf(line)}$	16 774	15 655	14 537	13 978	12 301	10 847
$C^{cust}_{wf(line)}$	61 551	59 299	58 549	55 546	52 168	45 788
LCC_{line}	85 808	82 842	81 378	78 220	73 970	66 948
	Cost in thousands of dollars					

cascading and 8% with no cascading. With 2 anchor towers, the effect of the cascading is to increase costs by 16%, and, as expected, the effect of including the cascading decreases as the number of anchor towers increases. Overall, the effects of including cascading and changing the number of anchor towers are modest.

However, if customer costs are considered, there is a dramatic increase in life cycle costs of about one order of magnitude. The trends have similar form as the case of no customer costs but the effect of more anchor towers is larger and the effect of including cascading is smaller: As the number of anchor towers increases from 2 to 9, the life cycle cost decreases by 24% with cascading and 19% with no cascading. With 2 anchor towers, the effect of the cascading is to increase costs by 11%.

In evaluating these results, it must be noted again that the cost estimates without customer costs are good estimates, whereas the cost

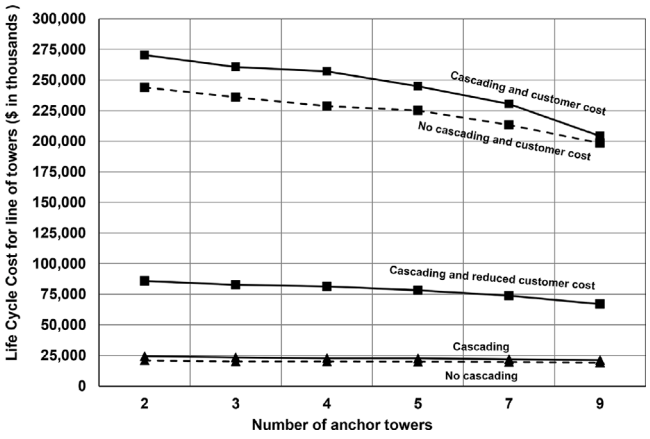

Fig. 10. Life cycle cost for a line of 25 towers considering different cases.

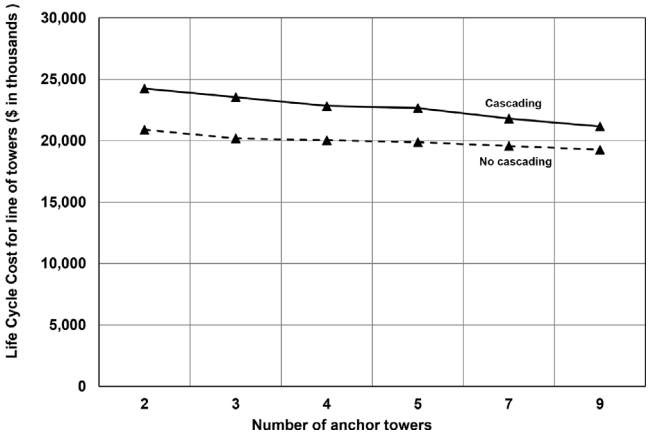

Fig. 11. Life cycle cost for a line of 25 towers excluding customer cost.

estimates for customer cost are very rough approximations, as discussed in Section 4.4. The results with customer costs vary considerably with the rough estimates. This sensitivity is illustrated in the last section of Table 4 by considering one quarter of the estimated customer costs, which would arise, for example, by changing the estimated fraction of transmission outages directly affecting customer outages from f_{ENS} = 20% to f_{ENS} = 5%, or by changing f_{ENS} = 20% to f_{ENS} = 10% and changing the customer outage cost from $C_{customer}$ = \$840,000 to $C_{customer}$ = \$420,000 per hour. The life cycle costs with no customer costs increase by a factor of about 2.5 when these reduced customer costs are included. The conclusion that customer costs dominate the life cycle costs remains. The large increase in costs when customer costs are considered highlights the importance of considering customer costs when estimating life cycle costs as well as the high priority that should be placed on greatly improving the very limited available data and methods for estimating customer costs.

Another trend that is visible from results in Figs. 10 and 11 and should be discussed in more detail is that the life cycle costs decrease with increase in the number of anchor towers. The analysis of life-cycle costs encompasses both direct and indirect costs. Indirect damages not only cover the direct expenses needed for line restoration but also include the costs related to the power loss experienced by customers. It is also evident from the results that these cumulative costs can become substantial (Fig. 10). Thus, to mitigate these indirect costs, installing more robust towers decreases the probability of cascade failures occurring in a line of towers. Such an approach decreases the likelihood of cascading failures along the line, consequently reducing the associated indirect costs stemming from outages. Thus, the most

effective strategy for mitigating cascade failure involves the installation of additional anchor towers. The authors identify several key concepts that significantly contribute to these findings. Firstly, for resilience assessment, there needs to be a balance between mitigation and recovery. This frequently poses a highly intricate challenge that necessitates comprehending how mitigation efforts affect the magnitude of damages and the potential costs and time required for recovery. Factors such as available resources and the impact of recovery time on customer losses are also key considerations in addressing this complex problem [58,59]. Many studies stress importance on mitigation measures due to unforeseen costs but the approach is not adopted by infrastructure owners due to risk acceptance and budgetary thresholds [60].

6. Conclusions

Under straight line winds, initial structural failures of transmission towers weaken the adjacent towers and can cause a cascade of further tower structural failures. This paper introduces the first probabilistic method to quantify the structural cascading failure of transmission towers due to straight line winds. First a single 500 kV transmission tower system (tower, insulators, cables) is dynamically analyzed to find its annual probability of failure under high winds when the adjacent towers are intact and when they are damaged.

Given these annual failure probabilities, novel mathematical formulas are derived for the probability distribution of the total number of towers failed and the mean number of towers failed. These formulas apply generally to cascading along a line of general components when the component failure probability is known when the adjacent components are intact and when an adjacent component is failed. The formulas are long but can be readily generated and evaluated using computer algebra. In particular, the effect of including anchor towers (assumed not to fail) in the line of towers can be determined. The detailed structural analysis combined with the cascading formulas are a new method to quantify how structural tower failures spread in a cascade. The method scales to apply to lines of dozens of towers and can handle different configurations of anchor towers that limit the cascading spread. Our methods can be applied generally, but as a specific illustration, the new cascading analysis is applied to a case study of a line of twenty-five 500 kV towers exposed to hurricane winds. The increased number of towers failing due to cascading is quantified with the change in the distribution of the number of failures and the increased mean number of failures. This analysis of probabilities is combined with construction, maintenance, and repair costs to illustrate how the life cycle cost of including cascading can be determined. In this case study, the cascading causes a modest increase in life cycle cost. Additional anchor towers limit the initial tower failures and the extent of the cascading and reduce the life cycle cost slightly.

Transmission tower failures can cause or prolong customer outages. One effect is that the extra time to repair additional failed towers in a line of towers can sometimes prolong customer outages. The resulting customer costs are currently hard to estimate, but we make rough estimates that suggest that when these customer costs are included, they dominate the life cycle costs. That is, the poorly known customer costs matter for transmission tower design and should be pursued in future research. In particular, improvements are needed in methods and data for estimating the impact and costs of transmission system outages on customers, especially under the extreme wind conditions that are a main cause of transmission system damage.

While the paper has made a major contribution in defining a probabilistic approach for the assessment of cascading failures along a line of transmission towers, the following limitations have been identified that could make the ground work for further research. In calculating the failure probabilities, the effects of pull down from adjacent failing towers or explicit dynamic analysis due to abrupt breakage of the conductors has not been considered. It is suggested that future research looking into the design of transmission towers accounts for such effects through high-fidelity dynamic analyses. Furthermore, this manuscript considered a single angle of wind attack and independence of wind speeds at different tower locations along the line. Prior work such as Alminhana et al. [14] has applied correlated wind fields to a case of cascading in a line of eight towers. Zeng et al. [61] discuss the generation of spatially correlated wind fields under a cyclone and present correlated fragility functions for a building using joint probability functions. In another study, Zeng et al. [62] apply spatially correlated cyclone fields to assess the damage to a power network considering uncertainties in wind loads and uncertainties in power network through fragility curves. Future work could use joint probability distributions for wind speed and direction along the line of transmission towers to generate failure probabilities for our probabilistic calculations that varied by tower. The variation of failure probabilities with wind direction could be accommodated simply by rerunning the calculations for different wind directions. However, the variation of failure probabilities by tower would increase the complexity of the formulas for the extent of the cascading but would be worth trying. The approximation of using an average value of failure probabilities could be assessed by comparing the cascading statistics of a short line of towers with varying failure probabilities with the cascading statistics of the same short line of towers with an average value of failure probabilities. The novel probabilistic approach to cascading transmission towers proposed in this paper is a strong start towards these future contributions.

CRediT authorship contribution statement

Saransh Dikshit: Writing – original draft, Visualization, Validation, Formal analysis, Data curation. **Ian Dobson:** Writing – review & editing, Validation, Methodology, Investigation, Conceptualization. **Alice Alipour:** Writing – review & editing, Supervision, Project administration, Methodology, Investigation, Funding acquisition, Conceptualization.

Declaration of competing interest

The authors declare the following financial interests/personal relationships which may be considered as potential competing interests: Alice Alipour reports financial support was provided by National Science Foundation. Ian Dobson reports financial support was provided by National Science Foundation.

Acknowledgments

We gratefully acknowledge funding from NSF, United States grants 1751844, 2302731, 1735354, and 2153163.

References

[1] Castillo A. Risk analysis and management in power outage and restoration: A literature survey. Electr Power Syst Res 2014;107:9–15.
[2] Ouyang M. Review on modeling and simulation of interdependent critical infrastructure systems. Reliab Eng Syst Saf 2014;121:43–60.
[3] Ekisheva S, Rieder R, Norris J, Lauby M, Dobson I. Impact of extreme weather on North American transmission system outages. IEEE Power Energy Soc Gen Meet 2021.
[4] Jacobs M. 13 Of the largest power outages in history - and what they tell us about the 2003 northeast blackout. 2013, https://blog.ucsusa.org/mike-jacobs/2003-northeast-blackout-and-13-of-the-largest-power-outages-in-history-199/.
[5] Dempsey D, White H. Winds wreak havoc on lines. Transm Distrib World 1996;48:32–42.
[6] Savory E, Parke GA, Zeinoddini M, Toy N, Disney P. Modelling of tornado and microburst-induced wind loading and failure of a lattice transmission tower. Eng Struct 2001;23(4):365–75.
[7] Wells J. Helicopters replace massive transmission lines toppled by hurricane michael. 2019, https://illumination.duke-energy.com/articles/helicopters-replace-massive-transmission-lines-toppled-by-hurricane-michael.
[8] North American Electric Reliability Corporation. Hurricane Harvey event analysis report. 2018.

[9] Ghannoum E. A rational approach to structural design of transmission line. IEEE Trans Power Appar Syst 1981;PAS-100(7):3506–12.
[10] Peabody AB, McClure G. Longitudinal design loads - A historical perspective. Electr Transm New Age 2002.
[11] McClure G, Tinawi R. Mathematical modeling of the transient response of electric transmission lines due to conductor breakage. Comput Struct 1987;26(1–2):41–56.
[12] Xue J, Mohammadi F, Li X, Sahraei-Ardakani M, Ou G, Pu Z. Impact of transmission tower-line interaction to the bulk power system during hurricane. Reliab Eng Syst Saf 2020;203:107079.
[13] Alminhana F, Mason M, Albermani F. A compact nonlinear dynamic analysis technique for Transmission Line Cascades. Eng Struct 2018;158:164–74.
[14] Alminhana F, Mason M, Albermani F. Transmission line failure propagation under extreme wind scenarios: Extratropical cyclones. Eng Struct 2023;284:115942.
[15] Han S-R, Guikema SD, Quiring SM, Lee K-H, Rosowsky D, Davidson RA. Estimating the spatial distribution of power outages during hurricanes in the Gulf Coast Region. Reliab Eng 2009;94(2):199–210.
[16] Winkler J, Duenas-Osorio L, Stein R, Subramaniam D. Performance assessment of topologically diverse power systems subjected to hurricane events. Reliab Eng Syst Saf 2010;95(4):323–36.
[17] Javanbakht P, Mohagheghi S. A risk-averse security-constrained optimal power flow for a power grid subject to hurricanes. Electr Power Syst Res 2014;116:408–18.
[18] Ouyang M, Duenas-Osorio L. Multi-dimensional hurricane resilience assessment of electric power systems. Struct Saf 2014;48:15–24.
[19] Cadini F, Agliardi GL, Zio E. Estimation of rare event probabilities in power transmission networks subject to cascading failures. Reliab Eng Syst Saf 2017;158:9–20.
[20] Zhou K, Cruise JR, Dent CJ, Dobson I, Wehenkel L, Wang Z, Wilson AL. Bayesian estimates of transmission line outage rates that consider line dependencies. IEEE Trans Power Syst 2021;36(2):1095–106.
[21] Gjorgiev B, Sansavini G. Identifying and assessing power system vulnerabilities to transmission asset outages via cascading failure analysis. Reliab Eng Syst Saf 2022;217:108085.
[22] Baldick R, et al. Initial review of methods for cascading failure analysis in electric power transmission systems. In: 2008 IEEE power and energy society general meeting. 2008, p. 1–8.
[23] Cavalieri F, Franchin P, Buritica Cortes J, Tesfamriam S. Models for seismic vulnerability analysis of power networks: comparative assessment. Comput Aided Civ Infrastruct Eng 2014;29(8):590–607.
[24] Dobson I, Carreras BA, Lynch VE, Newman DE. Complex systems analysis of series of blackouts: Cascading failure, critical points, and self-organization. Chaos 2007;17(2):026103.
[25] Bialek J, et al. Benchmarking and validation of cascading failure analysis tools. IEEE Trans Power Syst 2016;31(6):4887–900.
[26] Cheng B, Nozick L, Dobson I. Investment planning for earthquake-resilient electric power systems considering cascading outages. Earthq Spectra 2022;38(3):1734–60.
[27] Mühlhofer E, Koks EE, Kropf CM, Sansavini G, Bresch DN. A generalized natural hazard risk modelling framework for Infrastructure Failure Cascades. Reliab Eng Syst Saf 2023;234:109194. http://dx.doi.org/10.1016/j.ress.2023.109194.
[28] Scherb A, Garre L, Straub D. Evaluating component importance and reliability of power transmission networks subject to windstorms: Methodology and application to the Nordic grid. Reliab Eng Syst Saf 2019;191.
[29] Park H-S, Choi BH, Kim JJ, Lee T-H. Seismic performance evaluation of high voltage transmission towers in South Korea. KSCE J Civ Eng 2015;20(6):2499–505.
[30] Liu J, Tian L, Meng X, Yang M. Seismic fragility assessment of a transmission tower considering mainshock-aftershock sequences. J Constr Steel Res 2022;194:107344.
[31] Tian L, Pan H, Ma R. Probabilistic seismic demand model and fragility analysis of transmission tower subjected to near-field ground motions. J Constr Steel Res 2019;156:266–75.
[32] Gong J, Zhi X. Earthquake failure mode and collapse fragility of a 1000 kv outgoing line frame considering interactions in the Tower Line System. Structures 2020;27:626–38.
[33] Pan H, Tian L, Fu X, Li H. Sensitivities of the seismic response and fragility estimate of a transmission tower to structural and ground motion uncertainties. J Constr Steel Res 2020;167:105941.
[34] Tian L, Yang M, Liu S, Liu J, Gao G, Yang Z. Collapse failure analysis and fragility analysis of a transmission tower-line system subjected to the multidimensional ground motion of different input directions. Structures 2023;48:1018–28.
[35] Tian L, Wang W, Ma R, Wang L. Progressive collapse analysis of power transmission tower under earthquake excitation. Open Civ Eng J 2013;7(1):164–9.
[36] Tian L, Ma R, Pan H, Qiu C, Li W. Progressive collapse analysis of long-span transmission tower-line system under multi-component seismic excitations. Adv Struct Eng 2017;20(12):1920–32.
[37] Fu X, Li H-N, Li G. Fragility analysis and estimation of collapse status for transmission tower subjected to wind and rain loads. Struct Saf 2016;58:1–10.
[38] Bi W, Tian L, Li C, Ma Z, Pan H. Wind-induced failure analysis of a transmission tower-line system with long-term measured data and orientation effect. Reliab Eng Syst Saf 2023;229:108875.
[39] Ma L, Christou V, Bocchini P. Framework for probabilistic simulation of power transmission network performance under hurricanes. Reliab Eng Syst Saf 2021;217:108072.
[40] Teoh YE, Alipour A, Cancelli A. Probabilistic performance assessment of power distribution infrastructure under wind events. Eng Struct 2019;197:109199.
[41] Dikshit S, Alipour A. A moment-matching method for fragility analysis of transmission towers under straight line winds. Reliab Eng Syst Saf 2023;236:109241.
[42] Shinozuka M, Deodatis G. Simulation of stochastic processes by spectral representation. Appl Mech Rev 1991;44(4):191–204.
[43] Shinozuka M, Jan C. Digital simulation of random processes and its applications. J Sound Vib 1972;25(1):111–28.
[44] Benowitz BA, Deodatis G. Simulation of wind velocities on long span structures: A novel stochastic wave based model. J Wind Eng Ind Aerodyn 2015;147:154–63.
[45] Alipour A, Sarkar P, Dikshit S, Razavi A, Jafari M. Analytical approach to characterize tornado-induced loads on lattice structures. J Struct Eng 2020;146(6).
[46] Jafari M, Sarkar PP. Wind-induced response characteristics of a yawed and inclined cable in ABL wind: Experimental- and numerical-model based study. Eng Struct 2020;214:110681.
[47] Yeo D, Lin N, Simiu E. Estimation of hurricane wind speed probabilities: Application to New York City and other coastal locations. J Struct Eng 2014;140(6).
[48] Zerva A. Spatial variation of seismic ground motions: Modeling and Engineering Applications. CRC Press; 2016.
[49] Transmission cost estimation guide. 2022, Midcontinent Independent System Operator.
[50] Cui W, Caracoglia L. Simulation and analysis of intervention costs due to wind-induced damage on tall buildings. Eng Struct 2015;87:183–97.
[51] KEMA. Connecticut siting council investigation into the life-cycle costs of electric transmission lines. 2012.
[52] Fenton GA, Sutherland N. Reliability-based transmission line design. IEEE Trans Power Deliv 2011;26(2):596–606.
[53] Panteli M, Pickering C, Wilkinson S, Dawson R, Mancarella P. Power system resilience to extreme weather: fragility modelling, probabilistic impact assessment and adaption measures. IEEE Trans Power Syst 2017.
[54] Allred C. 5 major benefits of drone power line inspections. 2023, URL https://thedronelifenj.com/benefits-of-drone-power-line-inspections/,
[55] Fausset R, Mervosh S, Rojas R. Hurricane updates: New orleans without power as Hurricane Ida Batters louisiana (published 2021). 2021, https://www.nytimes.com/live/2021/08/29/us/ hurricane-ida-live-updates-new-orleans-louisiana.
[56] Wikipedia. Harmonic number. 2023, URL https://en.wikipedia.org/wiki/Harmonic_number.
[57] Zekavati AA, Jafari MA, Mahmoudi A. Regional multihazard risk-assessment method for overhead transmission line structures based on failure rate and a Bayesian updating scheme. J Perform Construct Facil 2023;37(1).
[58] Zhang N, Alipour A. A stochastic programming approach to enhance the resilience of infrastructure under weather-related risk. Comput-Aided Civ Infrastruct Eng 2022;38(4):411–32.
[59] Zhang N, Alipour A. A multi-step assessment framework for optimization of flood mitigation strategies in transportation networks. Int. J. Disaster Risk Reduct. 63:102439.
[60] Porter K, Scawthorn C. Estimating the benefits of climate resilient buildings and core public infrastructure. Institute for catastrophic loss reduction research paper series, vol. 65, 2020, p. 35.
[61] Zeng D, Zhang H, Wang C. Modelling correlated damage of spatially distributed building portfolios under scenario tropical cyclones. Struct Saf 2020;87:101978.
[62] Zeng D, Zhang H, Quanwang L, Ellingwood BR. Tropical cyclone damage assessment of distributed infrastructure systems under spatially correlated wind speed. Struct Saf 2021;91:102080.